Multi-decadal stability of water ages and tracer transport in a temperate-humid river basin

Wang, Siyuan; Hrachowitz, Markus; Schoups, Gerrit; Störiko, Anna

DOI
10.1088/1748-9326/ada8c1

Publication date
2025

Document Version
Final published version

Published in
Environmental Research Letters

ENVIRONMENTAL RESEARCH
LETTERS

LETTER • OPEN ACCESS

Multi-decadal stability of water ages and tracer transport in a temperate-humid river basin

To cite this article: Siyuan Wang *et al* 2025 *Environ. Res. Lett.* **20** 024046

IOP Publishing Environ. Res. Lett. 20 (2025) 024046 https://doi.org/10.1088/1748-9326/ada8c1

ENVIRONMENTAL RESEARCH
LETTERS

OPEN ACCESS

RECEIVED
27 July 2024

REVISED
28 November 2024

ACCEPTED FOR PUBLICATION
10 January 2025

PUBLISHED
30 January 2025

LETTER

Multi-decadal stability of water ages and tracer transport in a temperate-humid river basin

Siyuan Wang[1,2,*], **Markus Hrachowitz**[1], **Gerrit Schoups**[1] and **Anna Störiko**[1]

[1] Department of Water Management, Faculty of Civil Engineering and Geosciences, Delft University of Technology, Stevinweg 1, 2628CN Delft, The Netherlands
[2] Faculty of Technology Water, Energy and Environmental Engineering, University of Oulu, Pentti Kaiteran katu 1, 8000 Oulu, Finland
[*] Author to whom any correspondence should be addressed.

E-mail: Siyuan.Wang@oulu.fi and S.Wang-9@tudelft.nl

Keywords: water ages, young water fractions, transport variability, temporal scales, hydrological model

Supplementary material for this article is available online

Abstract

The temporal dynamics of water ages provide crucial insights into hydrological processes and transport mechanisms, yet there remains a significant gap in quantifying water age variability across different temporal scales. This study utilizes a comprehensive dataset spanning 70 years of hydrological observations and tritium records (1953–2022) with a semi-distributed hydrological model with integrated tracer routing routine based on StorageAge Selection functions SAS, to explore the temporal evolution of water ages in the 4000 km^2 Upper Neckar River basin, Germany. Our findings indicate a systematic convergence of the variability of young water fractions and other metrics of water age in riverflow and evaporation towards stable values when averaging over increasing time scales. While at daily scales exhibiting considerable variability with young water fractions in riverflow $F_{\mathrm{wy,Q}} \sim 0.01$–0.91 and in evaporation $F_{\mathrm{wy,E}} \sim 0.02$–0.75, the variability of $F_{\mathrm{wy,Q}}$ and $F_{\mathrm{wy,E}}$ gradually reduces with increasing averaging time scales and converge to 0.45–0.47 and 0.96–0.97, respectively, between individual decades. Liquid water input (P_{L}), comprising rainfall and snow melt, emerges as the dominant driver of $F_{\mathrm{wy,Q}}$ across all time scales. In contrast, $F_{\mathrm{wy,E}}$ shows varying controls with time scale: soil moisture content governs daily fluctuations, whereas P_{L} dominates at the decadal scale. Overall, water ages demonstrate remarkable stability with only minor deviations in response to climatic variability: a 20% fluctuation in average decadal P_{L} results in only ∼4% variation in $F_{\mathrm{wy,Q}}$ and ∼1% in $F_{\mathrm{wy,E}}$ over the study period. These findings suggest a lack of major long-term dynamics in water ages. Consequently, the results suggest that the physical transport dynamics in the Upper Neckar River basin, and potentially in comparable river basins with similar water age characteristics, can be considered near-stationary over multiple decades.

1. Introduction

As the crucial link between hydrology and water quality at the catchment scale, water ages and distributions thereof (i.e. transit time distributions; TTDs) are a metric of physical transport through a hydrological system (Hrachowitz *et al* 2016). As such they are a descriptor of how water and, as a consequence, nutrients and pollutants are stored in and released from catchments via different flow paths (Rinaldo *et al* 2015, Sprenger *et al* 2018, Benettin *et al* 2022).

The celerity-driven hydrological response, including riverflow and evaporation, acts at different time scales than the velocity-driven TTDs that underlie the water quality response in catchments (Weiler *et al* 2003, McDonnell and Beven 2014, Hrachowitz *et al* 2016). Temporal variability of the hydrological response over a spectrum of time-scales from minutes to multiple decades has been extensively described in literature (Thompson and Katul 2012, Berghuijs *et al* 2014, Sivapalan and Blöschl 2015, McMillan 2020, Berghuijs and Slater 2023). In contrast, the majority of studies that seek to analyse temporal variability of water ages and the underlying drivers have so far focused on daily time scales. These studies demonstrate that water ages in fluxes such as riverflow or evaporation, can fluctuate considerably at this time scale and that the main driver behind this variability is the available water supply and the associated magnitude of precipitation input at that time scale (Benettin *et al* 2015, 2017, Harman 2015, Hrachowitz *et al* 2015, Soulsby *et al* 2016, Rodriguez *et al* 2018, Kuppel *et al* 2020, Wilusz *et al* 2020). Beyond that, several studies have reported significant, albeit attenuated variability at time scales from monthly (Kaandorp *et al* 2018, Knapp *et al* 2019, Stockinger *et al* 2019) over seasonal (Birkel *et al* 2016, Remondi *et al* 2018) to yearly (Heidbüchel *et al* 2013, Birkel *et al* 2015, Wilusz *et al* 2017, von Freyberg *et al* 2018, Stockinger and Stumpp 2024). At these scales, switches between distinct storage compartments, such as the unsaturated root-zone or the groundwater, as dominant source of water can become an additional factor regulating variability of water ages (Hrachowitz *et al* 2013).

However, as a result of insufficiently long tracer records in many catchments, there is only a handful of studies that have analysed water ages over time periods longer than 10–20 years (Hrachowitz *et al* 2010, Wang *et al* 2023). Thus, little is known about the variability over such longer time scales and the resulting long-term dynamics of water ages, including potentially systematic trends over time arising therefrom. This is in particular concerning as there is evidence that changes in land management and the associated changes to (sub-)surface flow paths and water storage volumes do affect water ages at such time scales (Danesh-Yazdi *et al* 2016, Hrachowitz *et al* 2021). Similarly, altered precipitation and atmospheric water demand due to climate change can, as 'external transport variability' (Kim *et al* 2016), directly impact water ages. As a consequence, catchment properties such as vegetation cover may adjust to a changing climate, potentially leading to additional changes in subsurface flow paths and/or water storage volumes (Wang *et al* 2024), as 'internal transport variability' (Kim *et al* 2016).

This knowledge gap increases uncertainties in our ability to predict removal of legacy solutes such as nitrate (Basu *et al* 2010, Howden *et al* 2011) or chloride (Hrachowitz *et al* 2015) over time-scales of several decades but also the mobilization of solutes at shorter time-scales, such as phosphorus (e.g. Dupas *et al* 2018) under changing environmental conditions. The problem would be further exacerbated if water ages are non-self-averaging. Such a non-self-averaging behaviour has been widely observed for tracer and solute concentrations in stream water and is related to the fractal scaling of these variables (Kirchner *et al* 2000, Hrachowitz *et al* 2009, Godsey *et al* 2010, Kirchner and Neal 2013, Aubert *et al* 2014). In non-self-averaging time series, the variability of their daily, monthly, yearly or decadal means remains constant or converges towards stable averages at rates lower than predicted by the central limit theorem. Such non-self-averaging time series can give rise to trends that can be robust but nevertheless artefacts and thus unreliable predictors of future solute dynamics, as demonstrated by Kirchner and Neal (2013).

The objective of this study is to quantify the temporal variability in water ages as well as to identify their dominant controls across time-scales from daily to multi-decadal and to analyse the associated temporal evolution of water ages for riverflow and evaporation in the Neckar River basin, Germany. The analysis is based on hydrological data and tritium records over a 70 year period (1953–2022) that we use together with a hydrological model with integrated tracer-routine to estimate water age distributions in riverflow and evaporation. More specifically, we test the hypotheses that (1) water ages of riverflow and evaporation are non-self-averaging and thus unpredictable over decadal time-scales, that (2) different drivers control variability of water ages at different time scales and that (3) water ages are subject to significant long-term dynamics on decadal time scales, reflecting hydro-climatic variability and associated changes in catchment (sub-)surface structure.

2. Study area and data

The study area is the 4000 km^2 Upper Neckar River basin in South-West Germany (figure 1 and supplementary material table S1). Briefly, the basin is characterized by a temperate-humid climate with long-term mean precipitation $P \sim 880$ mm yr^{-1} and temperature $T \sim 8.2$ °C. Summer precipitation of $\sim$500 mm yr^{-1} (May–October) is balanced by winter precipitation of $\sim$380 mm yr^{-1} (November–April), respectively (figure S1). The landscape is characterized by terrace-like elements, undulating hills and steep and narrow forested valleys in the uplands (figure 1(c)).

For the analysis we used daily hydro-meteorological data for the time period 01/01/1953–31/12/2022 from the German Weather Service (DWD) and the German Federal Institute of Hydrology (BfG) (figure S1). Daily potential evaporation E_P (mm d^{-1}) was estimated using the Hargreaves equation. Daily riverflow records were available for the same time period at the basin outlet at Plochingen and for three additional nested sub-catchments (figure 1(a)) from the BfG. Tritium (^{3}H) data in precipitation and riverflow were available from the stations Stuttgart and Obertürkheim close to the

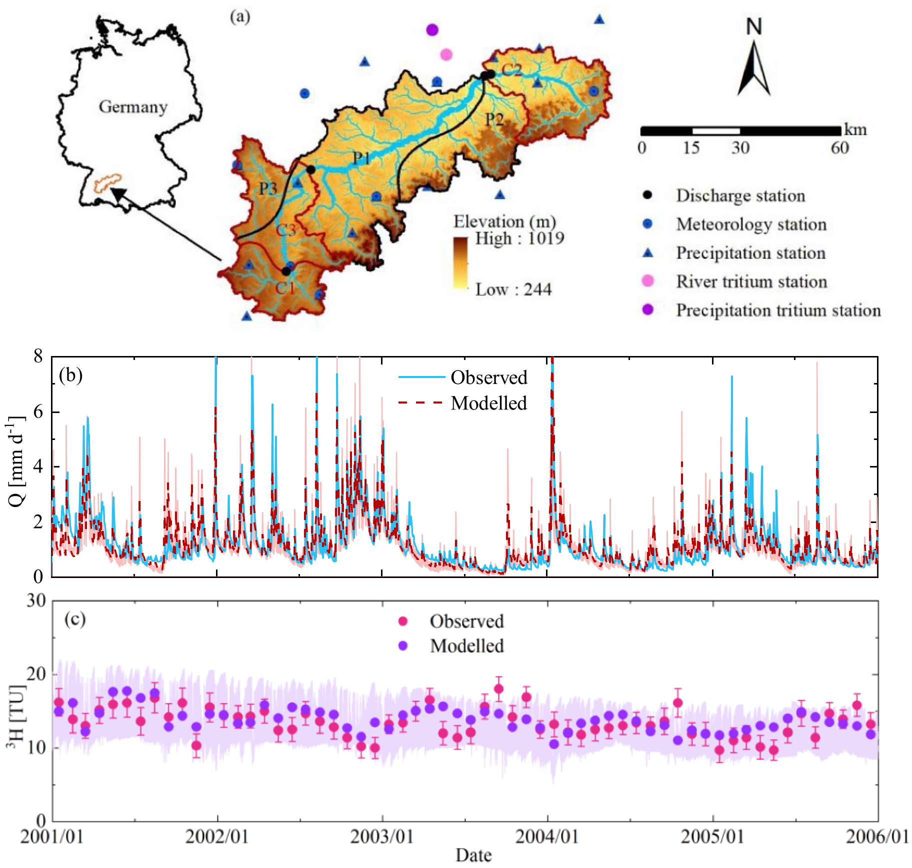

Figure 1. (a) Elevation of the Neckar catchment with discharge and hydro-meteorological stations as well as the water sampling locations in this study, three distinct precipitation zones P1—P3 (black outline), and three sub-catchments (red outlines; C1:Rottweil, C2:Plochingen at Fils, C3:Horb) within the upper Neckar basin, (b) selected part of the time series of observed (blue line) and modelled daily riverflow (Q) from 01/01/2001 to 01/01/2006, where the red dashed line indicates modelled Q for the best solution, and the red shaded area the 5th/95th inter-quantile range obtained from all pareto optimal solutions, (c) selected time series of observed (pink dots) river ^{3}H signals with the error bars and modelled river ^{3}H signals from 01/01/2001 to 01/01/2006, where purple dots indicate the modelled river ^{3}H signal for the best solution and the light purple shaded area indicates the 5th/95th inter-quantile range of all retained pareto optimal solutions.

basin outlet for the period 1978–2018 (figure S1) from the Global Network of Isotopes in Precipitation and the BfG (Schmidt *et al* 2020). For the preceding 1953–1977 period the precipitation record was reconstructed by bias- correcting data from stations Vienna and Ottawa. A more detailed description of the study region and the data used can be found in the supplementary material and in Wang *et al* (2023), (2024)).

3. Methods

We used a semi-distributed process-based hydrological model, which has previously been implemented and tested for the study basin (Wang *et al* 2023, 2024) and other environments world-wide (e.g. Prenner *et al* 2018, Hulsman *et al* 2021a, 2021b, Hanus *et al* 2021), based on the DYNAMIT modular modelling scheme (Hrachowitz *et al* 2014). Briefly, this model features three parallel hydrological response units, i.e. forest, grass/cropland and wetland, which are linked through a common storage component representing the groundwater system (figure S2). Overall, the model consists of an elevation-stratified snow storage (S_{snow}) as well as individual interception (S_i), unsaturated root zone (S_u), fast responding (S_f) and slow responding groundwater storage (S_s) components for each hydrological response unit.

The storage-age selection function (SAS) approach (e.g. Rinaldo *et al* 2015) was integrated with the hydrological model to route ^{3}H fluxes through the model. Briefly, each storage component used a uniform distribution as SAS function. Although this entails that each storage is fully mixed, the different time-scales of the individual storage components, lead to a 'combined' SAS functions that does not result in an overall fully mixed system response. The passive water storage $S_{s,p}$ (mm), characterized by $dS_{s,p}/dt = 0$, that physically represents groundwater volumes below the level of the river bed (Zuber 1986), was added as parameter to the active groundwater storage S_s for a sufficiently large mixing volume (Birkel *et al* 2011, figure S2).

Note that while the outflow Q_s from the groundwater storage is exclusively regulated by the active storage volume in S_s (equation (S6)), the ^{3}H of that outflow is sampled from the total groundwater storage volume $S_{s,tot} = S_s + S_{s,p}$.

Following a multi-objective strategy to ensure a plausible representation of model internal processes, the model was calibrated to simultaneously reproduce seven river flow signatures and river water ^{3}H dynamics. To reflect the vegetation adapting its active root system to changing climatic conditions during the 70 year study period, we independently estimated the model root-zone storage capacity parameter S_{umax} for each decade, as described by Wang *et al* (2024) and accordingly hardcoded the different values of S_{umax} in the model, varying between 95 and 115 mm throughout the study period. Tracking the ^{3}H signals, through the model allowed us to estimate the distributions of water ages in riverflow (Q) and actual evaporation, which here is the sum of interception evaporation and transpiration ($E = E_i + E_t$).

We used young water fractions (F_{wy}), i.e. water younger than 3 months (Kirchner 2016), as robust descriptor to describe water ages in the main text. The results of other age metrics, such as F_{w10}, i.e. fraction of water younger than 10 years, is provided in the supplementary material.

Detailed descriptions of the model implementation and calibration in the study region are provided by Wang *et al* (2023), (2024)) and in the supplementary material together with the model equations (table S2).

4. Results and discussion

The model reproduces the main features of the hydrological response over the entire study period, both at the basin outlet (figure 1(b), supplementary figure S3; table S5) and, as model test without further recalibration, in three nested sub-catchments (figure S4). It does not only capture the timing of flows (figure S3(a)), but also simultaneously reproduces well other observed riverflow signatures including the flow-duration curves (figure S3(d)), seasonal runoff coefficients (figure S3(c)) and autocorrelation functions (figure S3(e)). Similar to a previous implementation in the greater study region by Wang *et al* (2023), the model also catures the overall decline of river water 3H levels with NSE3H >0.93. In spite of somewhat underestimating peaks, the magnitude of seasonal 3H amplitudes and intra-annual fluctuations are represented well (figures 1(c), S5).

4.1. How do water ages vary over different time scales?

Tracking water fluxes through the model, a median non flow-weighted fraction of young water $F_{wy,Q} \sim 0.34$ emerged for riverflow on a daily time scale. At the same time, a pronounced variability with daily $F_{wy,Q}$ fluctuating between 0.01 and 0.91 (5th/95th percentile) was observed, reflecting differences in daily precipitation and evaporation (figures 2(a) and (b)). Describing older river water, daily $F_{w10,Q}$ varied between 0.41 and 0.95 and thus to a lesser degree in response to changing daily hydroclimatic conditions (figures 2(a) and (b)). To analyse the variability of water ages at different time scales, we computed block averages of F_{wy}, aggregating to weekly, monthly, seasonal, yearly and decadal values. With increasing averaging time scales, a reduction of variability was found. While average monthly $F_{wy,Q}$ oscillates between 0.02 and 0.75, this is eventually reduced to 0.44–0.47 for decadal averages with similarly reduced variability for $F_{w10,Q}$ (figure 2(a),b) and other age fractions (table S6). The observed convergence towards increasingly stable water ages is an indicator for a self-averaging process. As robust quantity to further test for self-averaging behaviour in the time series of water ages we plotted the root mean square differences (RMSD) of pairs of adjacent averages against the time interval n over which the averages were computed (figure 2(c)) as suggested by Kirchner and Neal (2013). It was found that at averaging time scales of >1 month, the rates of convergence of both $F_{wy,Q}$ and $F_{w10,Q}$ come close to $n^{-0.5}$, which describes a self-averaging and thus stationary process (e.g. white noise) as dictated by the central limit theorem. Such a process is characterized by weak persistence and thus little long-term fluctuations in water ages at low frequencies over time that here applies to time scales of at least multiple decades.

Evaporation is characterized by a markedly different age structure that is dominated by much younger water as illustrated by median $F_{wy,E} \sim 0.96$ and $F_{w10,E} > 0.99$, respectively. The daily $F_{wy,E}$ ranges from 0.56 to 1, while fractions of older water do not decrease below $F_{w10,E} \sim 0.75$ and thus exhibit less variability (figures 2(d) and (e)). Similar to riverflow, the variability in evaporation ages decreases with increasing averaging time scales (table S7), as illustrated by average monthly $F_{wy,E}$ that ranges from $\sim$0.81–1 which further decreases to a range of 0.96–0.97 for decadal averages (figures 2(d) and (e)). Correspondingly, the traces of RMSD of adjacent means as function of the averaging time scale n for both $F_{wy,E}$ and $F_{w10,E}$ show convergence rates close to $n^{-0.5}$ at averaging time scales larger than 6 months (figure 2(f)). This suggests that the age structure of evaporation is not subject to major long-term fluctuations and can thus also be assumed stationary at multi-decadal time scales.

4.2. What are the hydro-climatic drivers of water age variability at different time scales?

To explore which factor can best explain variability in F_{wy} regression analysis was used. For the

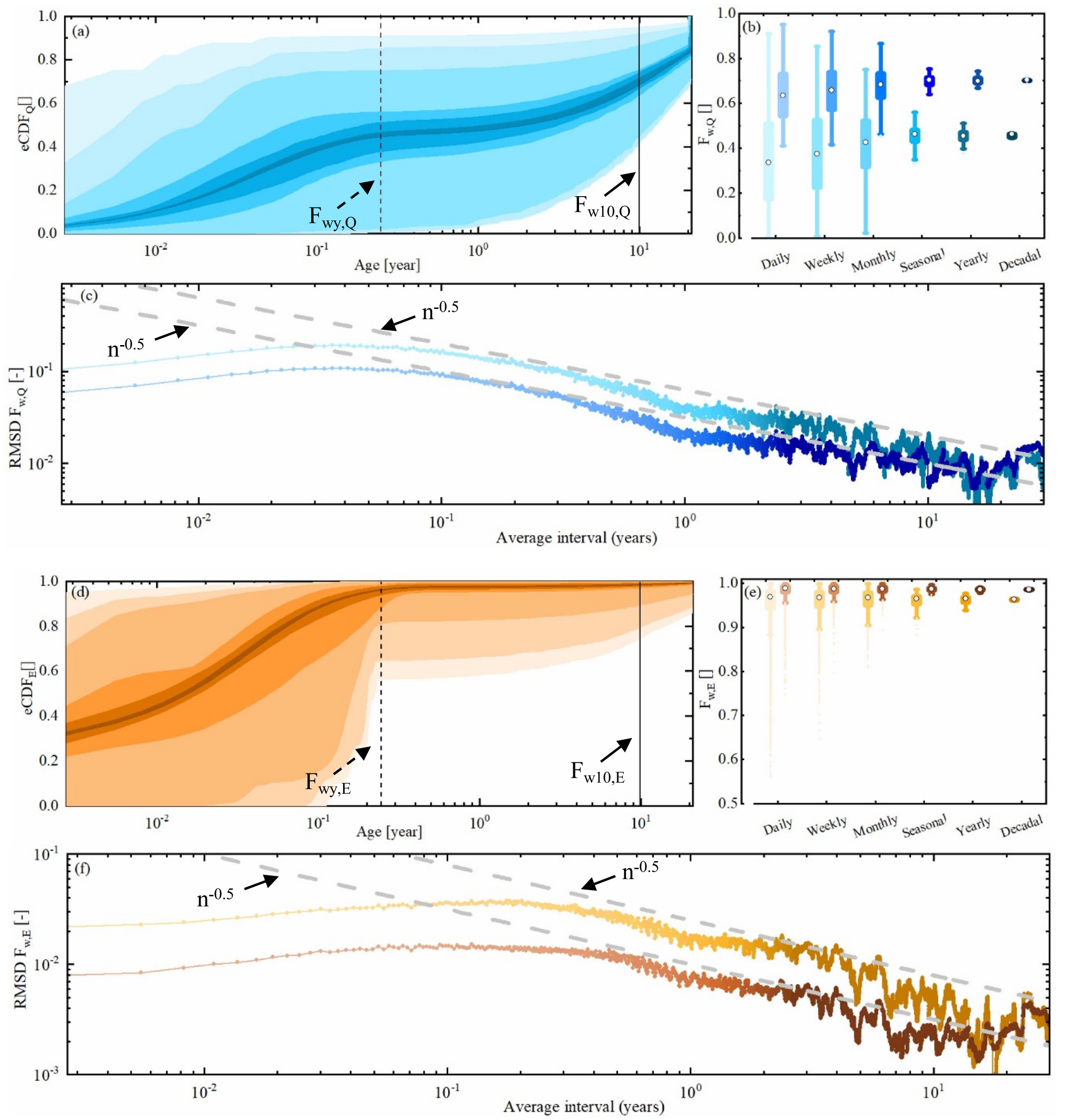

Figure 2. The variability of river flow TTDs (eCDF$_Q$) and evaporation TTDs (eCDF$_E$) from the most balanced model solution over various time scales. (a) The blue shades from lighter to darker indicate the 5th/95th intervals of the eCDF$_Q$ of the river water age distributions from daily to decadal averaging time-scales, (b) the blue and navy blue box plots (whiskers indicate 5th/95th percentiles) from lighter to darker indicates $F_{wy,Q}$ and $F_{w10,Q}$ from daily to decadal, respectively, (c) Root mean squared differences (RMSD) between pairs of successive average values in $F_{wy,Q}$ (the gradient blue line) and $F_{w10,Q}$ (the gradient navy blue line) plotted against corresponding averaging intervals, (d) the orange shades from lighter to darker indicate the eCDF$_E$ of the evaporation water age distributions from daily to decadal, (e) the yellow and brown boxes from lighter to darker indicates $F_{wy,E}$ and $F_{w10,E}$ from daily to decadal, respectively, (f) RMSD in $F_{wy,E}$ (the gradient yellow line) and $F_{w10,E}$ (the gradient brown line). Note that the dashed grey line is the slope of −0.5 predicted by the central limit theorem for self-averaging time series and n is the number of averaging time steps (here: years).

entire 70 year study period 1953–2022, the pronounced variability of young water fractions in riverflow $F_{wy,Q}$ at a daily time-scale is to first order controlled by daily liquid water input $P_L = P_{rain} + M_{snow}$ (figure 3(a)). This is illustrated by the sensitivity (ψ) of $F_{wy,Q}$ to P_L, approximated by a linear relationship $\psi = \Delta F_{wy,Q}/\Delta P_L \sim 0.03$ ($R^2 = 0.34$). Other potential hydro-climatic drivers, including Q as aggregate metric of catchment wetness ($R^2 = 0.22$), evaporation E ($R^2 = 0.22$) or root-zone moisture content S_u ($R^2 = 0.20$) exert weaker controls on $F_{wy,Q}$. Across all tested averaging time-scales, P_L remains the strongest driver, reaching $R^2 = 0.89$ with a sensitivity $\psi \sim 0.07$ at the decadal time-scale. P_L also becomes relatively more important compared to the other hydro-climatic variables ($R^2 = 0.25$–0.82; figure 3). At the seasonal time-scale it is notable that $F_{wy,Q}$ is somewhat more sensitive to P_L in winter ($\psi \sim 0.10$) than in summer ($\psi \sim 0.07$). Further analysis revealed that this effect can be attributed to the influence of winter snow melt. Periods of snow cover preceding snow melt, are characterized by low $F_{wy,Q} \sim 0.2$, on

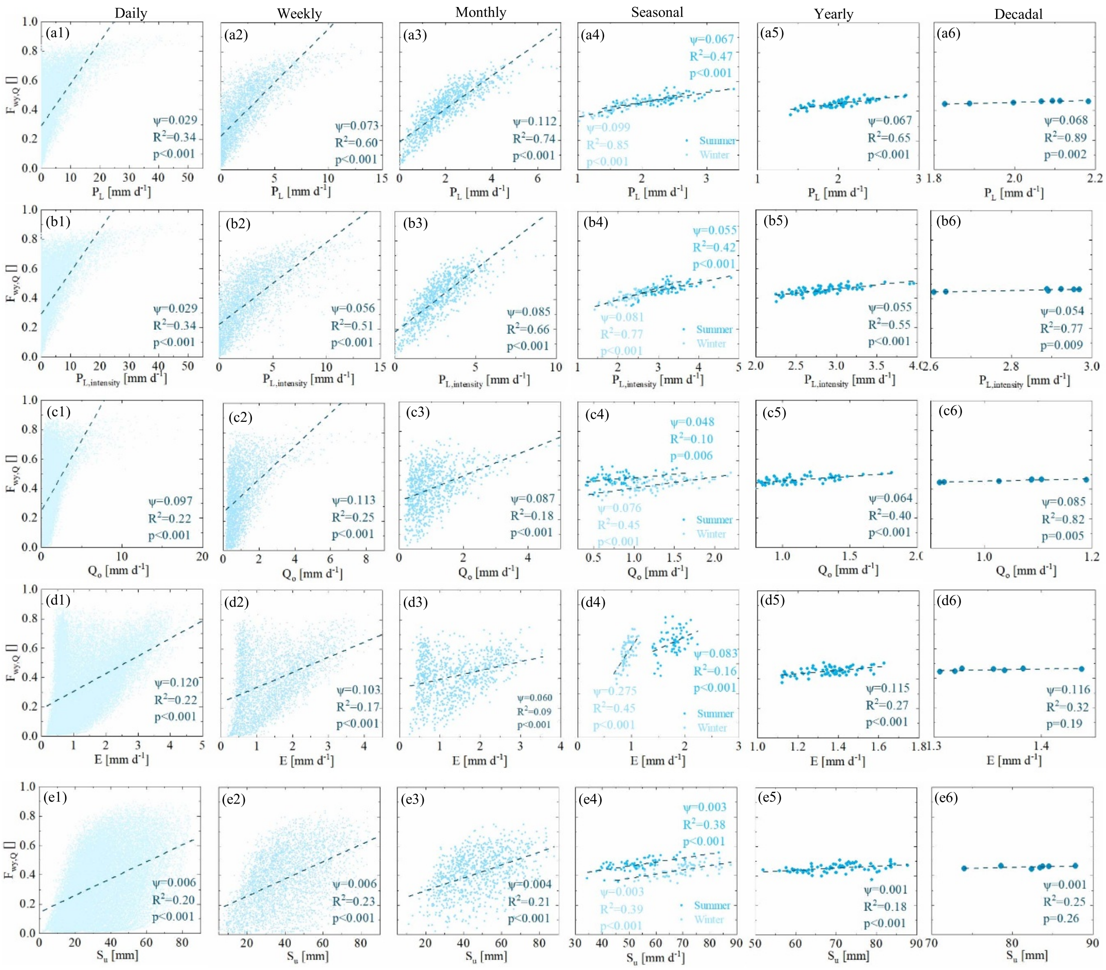

Figure 3. Relationship between the young water fraction in river flow ($F_{wy,Q}$) and hydro-climatic variables over different time scales from daily to decadal including (a) liquid precipitation P_L (rainfall +snowmelt), (b) liquid precipitation intensity $P_{L,intensity}$, (c) river flow Q_o, (d) evaporation E (e) soil moisture S_u. The dashed lines indicate the linear relationships between the $F_{wy,Q}$ and the various hydro-climatic variables x, used to approximate the sensitivity $\psi = \Delta F_{wy,Q}/\Delta x$.

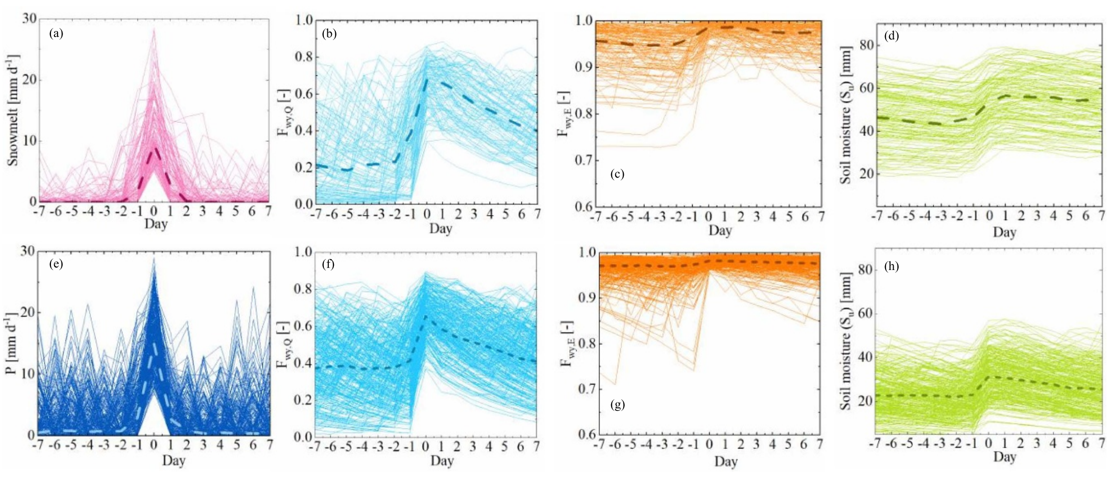

Figure 4. Sensitivity analysis of variability of the young water fractions (<3 months) in river flow ($F_{wy,Q}$)and evaporation ($F_{wy,E}$) as well as soil moisture S_u in response to the selected snowmelt events in winter in (a)–(d) and rainfall events in summer in (e)-(h).

average (figure 4(b)). Snow melt water is rather young as the presence of snow over periods longer than a few weeks is rare in the study region. As a consequence, snow melt inputs (figure 4(a)) increase $F_{wy,Q}$ to ~0.7. In contrast, $F_{wy,Q}$ preceding summer rainfall events (figure 4(e)) is, on average, with $F_{wy,Q} \sim 0.4$ considerably higher (figure 4(f)), due to frequent summer rain events. Although summer $F_{wy,Q}$ also reaches ~0.7, the

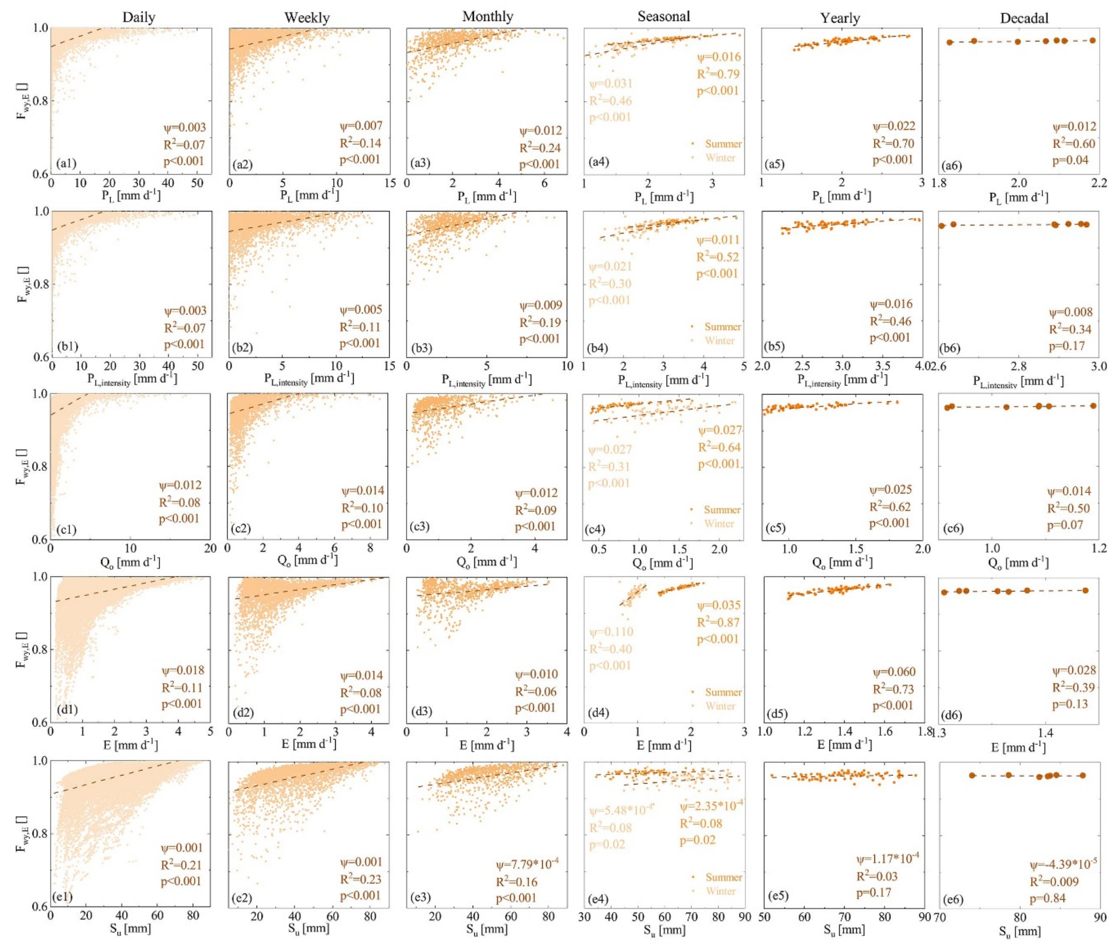

Figure 5. Relationship between the young water fraction in evaporation ($F_{\mathrm{wy,E}}$) and hydro-climatic variables over different time scales from daily to decadal including (a) liquid precipitation P_{L} (rainfall+snowmelt), (b) liquid precipitation intensity $P_{\mathrm{L,intensity}}$, (c) river flow Q_o, (d) evaporation E and (e) soil moisture S_u. The dashed lines indicate the linear relationships between the $F_{\mathrm{wy,E}}$ and the various hydro-climatic variables x, used to approximate the sensitivity $\psi = \Delta F_{\mathrm{wy,E}}/\Delta x$.

rate of increase from 0.4 to 0.7, and thus its sensitivity, is lower. Overall, controls on fractions of older water $F_{\mathrm{w10,Q}}$ correspond to those above with P_{L} being the strongest control on $F_{\mathrm{w10,Q}}$ (figure S6).

The variability in daily young water fraction in evaporation $F_{\mathrm{wy,E}}$ is driven to a lesser degree by liquid water input P_{L} ($R^2 = 0.07$; $\psi \sim 3 \cdot 10^{-3}$), but is more dependent on soil moisture S_u ($R^2 = 0.21$, $\psi \sim 10^{-3}$; figure 5). Aggregating the history of water input and release over the past weeks, S_u captures the interaction between water supply and atmospheric water demand. However, with increasing averaging time-scale the strength of S_u as driver gradually reduces to $R^2 < 0.01$ ($\psi \sim 10^{-5}$). Instead, E exhibits the strongest relation with $F_{\mathrm{wy,E}}$ at seasonal scale, with P_{L} emerging as dominant control on $F_{\mathrm{wy,E}}$ at the decadal time-scale ($R^2 = 0.60$; $\psi \sim 0.01$). This switch from S_u over E to P_{L} as dominant control illustrates that the history of water supply and release interactions in S_u preserves merely the system's memory of the past few weeks. At time-scales longer than that, the water fluxes released from the system become better predictors, while over decadal time-scales variations in water supply, expressed as P_{L}, control fluctuations in $F_{\mathrm{wy,E}}$. It can also be observed that at seasonal time-scale, $F_{\mathrm{wy,E}}$ is more sensitive to P_{L} and E in winter than in summer (figure 5). For P_{L}, this difference is explained by the higher sensitivity of $F_{\mathrm{wy,E}}$ to winter snow melt (figure 4(c)) than to summer rainfall (figure 4(g)), similar to $F_{\mathrm{wy,Q}}$. Low evaporation due to low temperatures together with little input of new liquid water during periods with snow cover cause water to remain in S_u longer, resulting in older ages during such periods (and thus lower $F_{\mathrm{wy,E}}$). With higher temperatures, snow melt and thus input of young water increases, accompanied by higher evaporation rates, that lead to quicker removal of water from S_u. This younger water that is evaporated at higher rates then leads to a faster turnover of water in S_u and thus to a distinct switch ($\psi \sim 0.11$) towards a younger water pool from which evaporation is sourced and the markedly higher $F_{\mathrm{wy,E}}$ (figure 5). Due

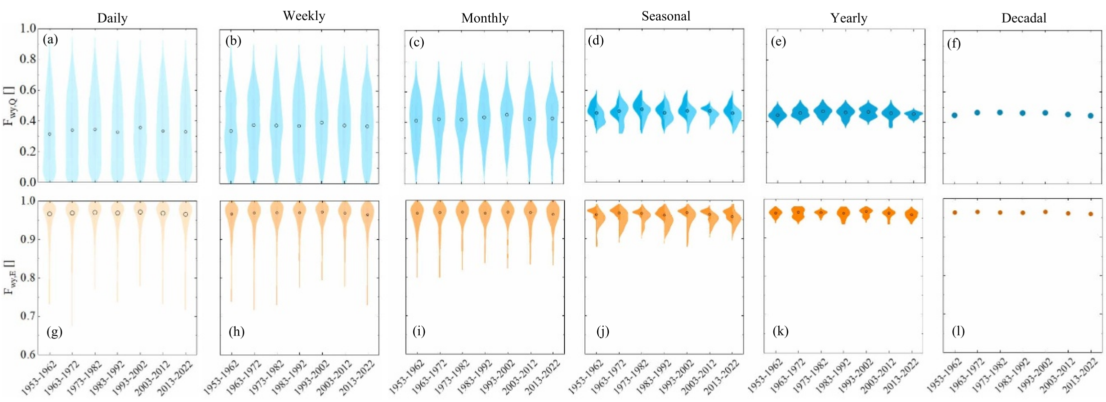

Figure 6. The differences of variability of the young water fractions in river flow ($F_{wy,Q}$, (a)–(f)) and evaporation ($F_{wy,E}$, (g)–(l)) over multi-decades for each time scale (from lighter to darker for daily to decadal). Note that the relatively darker and lighter colour shades in (d) and (j) indicate the F_{wy} in summer (May–October) and winter months (November—April), respectively.

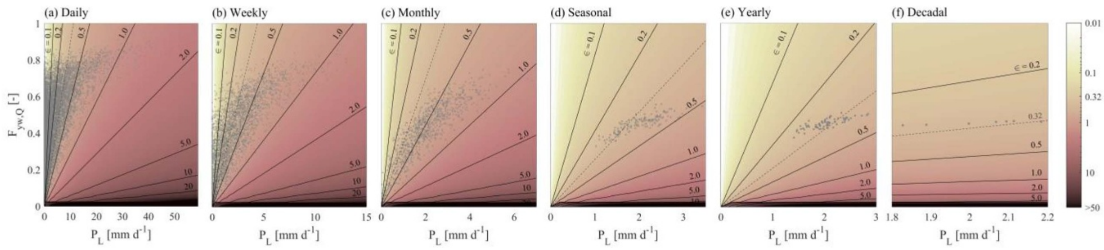

Figure 7. Elasticities, expressed as $\epsilon = \psi \cdot (P_L/F_{wy,Q}) = (\Delta F_{wy,Q}/F_{wy,Q})/(\Delta P_L/P_L)$ for (a) daily, (b) weekly, (c) monthly, (d) seasonal, (e) yearly and (f) decadal time-scales. Note that here ψ is obtained as least square fit to the data points (see figure 3(a)) representing the relationship between P_L and $F_{wy,Q}$ over different time scales from daily to decadal respectively (grey dots). The colour shading and black lines indicate various theoretical elasticity levels, the dashed grey lines indicate the highest elasticity $\epsilon = 0.32$ in the estimated water ages at decadal time-scale. Briefly, an elasticity of $\epsilon = 1$ implies that a 1% increase in $F_{yw,Q}$ (i.e. $\Delta F_{wy,Q}/F_{wy,Q} = 0.01$) follows from a 1% increase in P_L (i.e. $\Delta P_L/P_L = 0.01$). In contrast, for example $\epsilon = 0.32$ implies a 0.32% increase in $F_{yw,Q}$ (i.e. $\Delta F_{wy,Q}/F_{wy,Q} = 0.0032$) in response to a 1% increase in P_L. At daily ($\epsilon \leqslant \sim 1.5$) to seasonal ($\epsilon \leqslant \sim 0.5$) time-scales, a considerable proportion of liquid water inputs resulted in higher elasticities ϵ than at decadal time scales ($\epsilon \leqslant 0.32$), i.e. the grey dots that plot on the right side of the dashed grey line in (a)–(e).

to the absence of snow, the fluctuation in summer $F_{wy,E}$ is more gradual, as evident by its lower sensitivity to E ($\psi \sim 0.03$). The controls on $F_{w10,E}$ are comparable to those of $F_{wy,E}$ (figure S7).

4.3. Temporal evolution and long–term dynamics of water ages

Over the seven study decades, remarkably stable water ages can be observed (figure 6). As a consequence of the above, the fluctuations of average riverflow water ages between the individual decades are very minor. The same is true for the inter-decadal variabilities around these average water ages, for which merely some limited changes in the extremes can be observed (e.g. figure 6(c)). In spite of higher absolute sensitivities to hydro-climatic variability at decadal ($\psi \sim 0.07$) than at daily time-scales ($\psi \sim 0.03$), the relative sensitivities or elasticities of $F_{wy,Q}$ to P_L, expressed by $\epsilon = \psi \cdot (P_L/F_{wy,Q})$, were for wide parts of the P_L-$F_{wy,Q}$ space much lower at the decadal time-scale ($\epsilon \leqslant \sim 0.32$) than at the daily time-scale ($\epsilon \leqslant \sim 1.5$; figure 7). This implies that while average inter-decadal P_L varied by ∼650–803 mm yr^{-1} and thus by ∼20%, $F_{wy,Q}$ varied between 0.45–0.47 and thus by only ∼4%. For evaporation $F_{wy,E}$ it was found that $\epsilon \sim 0.11$, which entails that the 20% fluctuation in P_L as dominant control led to a $F_{wy,E}$ fluctuation of merely ∼2%, making average $F_{wy,E}$ similarly stable throughout the study period, (figures 6(g)–(i)).

4.4. Implications

The general magnitudes of $F_{wy,Q}$ and $F_{wy,E}$ from this study are broadly consistent with previous studies (von Freyberg *et al* 2018, Asenjan and Danesh-Yazdi 2020, Ceperley *et al* 2020). Our results also qualitatively correspond with previous studies that report reductions in water age variability for timescales from daily to yearly (Wilusz *et al* 2017) and up to 8 years (Stockinger and Stumpp 2024).

As first study to analyse water ages over multiple decades we have found no evidence for pronounced non-self-averaging behaviour. The limited fluctuation of decadal $F_{wy,Q}$ and $F_{wy,E}$ in response to the ∼20% variation in P_L and significant 10% increase in E_P over the 70 year study period suggests that the study basin buffers water ages against long-term hydro-climatic variability so that water ages and the associated conservative physical transport processes do not exhibit major long-term dynamics and can thus be assumed near-stationary at decadal time-scales with limited 'external transport variability' (Kim *et al* 2016). Wang *et al* (2024) have shown that vegetation adaptation to inter-decadal hydro-climatic variability in the study basin led to fluctuations in root-zone storage capacities, represented by parameter $S_{u,max}$ in our model. In spite of accounting for the fluctuations of this catchment subsurface property in our analysis $F_{wy,Q}$ and $F_{wy,E}$ remained remarkably insensitive to these changes. This therefore also indicates limited 'internal transport variability', which is consistent with the very minor changes to $F_{wy,Q}$ from 0.12 to 0.13 as a result of deforestation that led to a >50% reduction in $S_{u,max}$ in a nearby catchment (Hrachowitz *et al* 2021).

The self-averaging and temporally stable water ages contrast with the fractal scaling and non-self-averaging behaviour that is frequently observed in dynamics of river water tracer and solute concentrations and that indicates the potential presence of long-term fluctuations or trends in solute circulation dynamics. In spite of several sources of uncertainty in the modelling process (Beven 2016), our findings that water ages are near-stationary suggest that long-term solute dynamics as manifest by their fractal scaling in many river basins are unlikely to arise from changes in conservative transport processes. Instead, long-term solute dynamics may emerge as an inherent consequence of anomalous transport and the associated heavy-tails of TTDs (Dentz *et al* 2023) in combination with other potential factors such as long-term changes in solute supply and/or mobilization. The latter may include variations in solute input (e.g. fertilizer application, solute concentration in precipitation) but also alterations of (bio-) geochemical transformation processes due to changing ambient conditions, such as temperature or soil water content that regulate for example mineral dissolution kinetics in the subsurface (e.g. Maher 2011, Li *et al* 2017) but also plant nutrient uptake (e.g. Marschner and Rengel 2023).

It can be expected that water ages may be more sensitive to hydro-climatic variability in catchments which are characterized by younger water, i.e. higher $F_{yw,Q}$, and thus faster physical transport processes. However, it is plausible to assume that physical transport processes in river basins with similar water age structure (Koeniger *et al* 2005, Stewart *et al* 2010, Visser *et al* 2019, Birkel *et al* 2020) may exhibit similarly low elasticity to hydro-climatic variability and thus only limited long-term dynamics.

Overall, there are two wider implications following from the results of this study. Firstly, predictions of future solute dynamics in riverflow over long-time scales may be more robust than the frequently observed fractal scaling in river solute concentrations may suggest if estimated based on water ages instead of on the solute time series themselves. Secondly, the low elasticity of water ages to variability in water supply and the resulting long-term stability of physical transport processes poses practical limits for mitigation and remediation measures of legacy contamination such as nitrate (Basu *et al* 2022) that may aim to alter not only reactive processes but also physical transport characteristics by interventions such as wetland restoration or land management.

To further improve accuracy of estimated water ages and their long-term dynamics, additional tracers that allow age tracing of older water, such as CFCs and SF6 (Stewart *et al* 2007, Molénat *et al* 2013, Solomon *et al* 2015), may prove valuable for future studies.

5. Conclusions

Based on hydro-climatic records and ^3H data we have analysed the variability of water ages, described by the fraction of young water in riverflow ($F_{yw,Q}$) and evaporation ($F_{yw,E}$), at daily to decadal time-scales in the Upper Neckar Basin, Germany over the 70 year period 1953–2022. The main findings of our study are the following:

(1) Riverflow is, on average, with $F_{wy,Q} \sim 0.4$ characterized by considerably older water than evaporation with $F_{wy,E} > 0.95$ across all time-scales.
(2) The variabilities of both, $F_{wy,Q}$ and $F_{wy,E}$ systematically decreases with increasing averaging time-scale: decadal average $F_{yw,Q}$ fluctuates merely between 0.45–0.47 and $F_{wy,E}$ between 0.96–0.97 between individual decades. This indicates that $F_{wy,Q}$ and $F_{wy,E}$ can be considered near-stationary across several decades. These results therefore provide no evidence to support the hypothesis that $F_{wy,Q}$ and $F_{wy,E}$ are non-self-averaging and unpredictable.
(3) Liquid water input P_L is the dominant driver of $F_{wy,Q}$ across all time-scales. In contrast, $F_{wy,E}$ is characterized by varying drivers: while soil moisture is the dominant control at daily time-scale, this switches to liquid water input P_L at the decadal time-scale. Thus the hypothesis that the dominant controls on F_{yw} vary across different time-scales can only be rejected for $F_{wy,Q}$.
(4) Average water ages were rather stable and subject to minor fluctuations over time. In response to a 20% fluctuation in decadal P_L, $F_{wy,Q}$ varied only by ~4% and $F_{wy,E}$ by ~1% over the study period. The hypothesis that water ages are subject to major long-term dynamics on decadal time scales in the study basin was therefore rejected.
(5) Overall, as first study to systematically analyse water ages over multiple decades, it demonstrates that there is no evidence for non-self-averaging and unpredictable behaviour in water

ages. Instead long-term average water ages were rather stable and subject to merely minor fluctuations in the Upper Neckar basin. Consequently, and in spite of hydro-climatic variablity, the associated physical transport processes can be assumed to be near-stationary across multiple decades.

Data availability statement

All data that support the findings of this study are included within the article (and any supplementary files).

Acknowledgment

We acknowledge financial support from China Scholarship Council (CSC).

ORCID iDs

Siyuan Wang https://orcid.org/0000-0002-9639-9241
Markus Hrachowitz https://orcid.org/0000-0003-0508-1017

References

Asenjan M R and Danesh-Yazdi M 2020 The effect of seasonal variation in precipitation and evapotranspiration on the transient travel time distributions *Adv. Water Resour.* **142** 103618

Aubert A H, Kirchner J W, Gascuel-Odoux C, Faucheux M, Gruau G and Mérot P 2014 Fractal water quality fluctuations spanning the periodic table in an intensively farmed watershed *Environ. Sci. Technol.* **48** 930–7

Basu N B *et al* 2010 Nutrient loads exported from managed catchments reveal emergent biogeochemical stationarity *Geophys. Res. Lett.* **37** L23404

Basu N B *et al* 2022 Managing nitrogen legacies to accelerate water quality improvement *Nat. Geosci.* **15** 97–105

Benettin P *et al* 2022 Transit time estimation in catchments: recent developments and future directions *Water Resour. Res.* **58** e2022WR033096

Benettin P, Bailey S W, Rinaldo A, Likens G E, McGuire K J and Botter G 2017 Young runoff fractions control streamwater age and solute concentration dynamics *Hydrol. Process.* **31** 2982–6

Benettin P, Rinaldo A and Botter G 2015 Tracking residence times in hydrological systems: forward and backward formulations *Hydrol. Process.* **29** 5203–13

Berghuijs W R and Slater L J 2023 Groundwater shapes North American river floods *Environ. Res. Lett.* **18** 034043

Berghuijs W, Woods R and Hrachowitz M 2014 A precipitation shift from snow towards rain leads to a decrease in streamflow *Nat. Clim. Change* **4** 583–6

Beven K 2016 Facets of uncertainty: epistemic uncertainty, non-stationarity, likelihood, hypothesis testing, and communication *Hydrol. Sci. J.* **61** 1652–65

Birkel C, Duvert C, Correa A, Munksgaard N C, Maher D T and Hutley L B 2020 Tracer-aided modeling in the low-relief, wet-dry tropics suggests water ages and DOC export are driven by seasonal wetlands and deep groundwater *Water Resour. Res.* **56** e2019WR026175

Birkel C, Geris J, Molina M J, Mendez C, Arce R, Dick J, Tetzlaff D and Soulsby C 2016 Hydroclimatic controls on non-stationary stream water ages in humid tropical catchments *J. Hydrol.* **542** 231–40

Birkel C, Soulsby C and Tetzlaff D 2011 Modelling catchment-scale water storage dynamics: reconciling dynamic storage with tracer-inferred passive storage *Hydrol. Process.* **25** 3924–36

Birkel C, Soulsby C and Tetzlaff D 2015 Conceptual modelling to assess how the interplay of hydrological connectivity, catchment storage and tracer dynamics controls nonstationary water age estimates *Hydrol. Process.* **29** 2956–69

Ceperley N, Zuecco G, Beria H, Carturan L, Michelon A, Penna D, Larsen J and Schaefli B 2020 Seasonal snow cover decreases young water fractions in high Alpine catchments *Hydrol. Process.* **34** 4794–813

Danesh-Yazdi M, Foufoula-Georgiou E, Karwan D L and Botter G 2016 Inferring changes in water cycle dynamics of intensively managed landscapes via the theory of time-variant travel time distributions *Water Resour. Res.* **52** 7593–614

Dentz M, Kirchner J W, Zehe E and Berkowitz B 2023 The Role of Anomalous Transport in Long-Term, Stream Water Chemistry Variability *Geophysical Research Letters* **50**

Dupas R, Minaudo C, Gruau G, Ruiz L and Gascuel-Odoux C 2018 Multidecadal trajectory of riverine nitrogen and phosphorus dynamics in rural catchments *Water Resour. Res.* **54** 5327–40

Godsey S E *et al* 2010 Generality of fractal 1/f scaling in catchment tracer time series, and its implications for catchment travel time distributions *Hydrol. Process.* **24** 1660–71

Hanus S, Hrachowitz M, Zekollari H, Schoups G, Vizcaino M and Kaitna R 2021 Future changes in annual, seasonal and monthly runoff signatures in contrasting Alpine catchments in Austria *Hydrol. Earth Syst. Sci.* **25** 3429–53

Harman C J 2015 Time-variable transit time distributions and transport: theory and application to storage-dependent transport of chloride in a watershed *Water Resour. Res.* **51** 1–30

Heidbüchel I, Troch P A and Lyon S W 2013 Separating physical and meteorological controls of variable transit times in zero-order catchments *Water Resour. Res.* **49** 7644–57

Howden N, Burt T, Mathias S, Worrall F and Whelan M 2011 Modelling long-term diffuse nitrate pollution at the catchment-scale: data, parameter and epistemic uncertainty *J. Hydrol.* **403** 337–51

Hrachowitz M, Benettin P, Van Breukelen B M, Fovet O, Howden N J, Ruiz L, van der Velde Y and Wade A J 2016 Transit times—The link between hydrology and water quality at the catchment scale *Wiley Interdiscip. Rev.* **3** 629–57

Hrachowitz M, Fovet O, Ruiz L, Euser T, Gharari S, Nijzink R, Freer J, Savenije H H G and Gascuel-Odoux C 2014 Process consistency in models: the importance of system signatures, expert knowledge, and process complexity *Water Resour. Res.* **50** 7445–69

Hrachowitz M, Fovet O, Ruiz L and Savenije H H 2015 Transit time distributions, legacy contamination and variability in biogeochemical 1/f α scaling: how are hydrological response dynamics linked to water quality at the catchment scale? *Hydrol. Process.* **29** 5241–56

Hrachowitz M, Savenije H, Bogaard T, Tetzlaff D and Soulsby C 2013 What can flux tracking teach us about water age distribution patterns and their temporal dynamics? *Hydrol. Earth Syst. Sci.* **17** 533–64

Hrachowitz M, Soulsby C, Tetzlaff D, Dawson J J C, Dunn S and Malcolm I 2009 Using long-term data sets to understand transit times in contrasting headwater catchments *J. Hydrol.* **367** 237–48

Hrachowitz M, Soulsby C, Tetzlaff D and Speed M 2010 Catchment transit times and landscape controls—does scale matter? Hydrological Processes *Int. J.* **24** 117–25

Hrachowitz M, Stockinger M, Coenders-Gerrits M, van der Ent R, Bogena H, Lücke A and Stumpp C 2021 Reduction of vegetation-accessible water storage capacity after deforestation affects catchment travel time distributions and increases young water fractions in a headwater catchment *Hydrol. Earth Syst. Sci.* **25** 4887–915

Hulsman P, Hrachowitz M and Savenije H H 2021a Improving the representation of long-term storage variations with conceptual hydrological models in data-scarce regions *Water Resour. Res.* **57** e2020WR028837

Hulsman P, Savenije H H and Hrachowitz M 2021b Learning from satellite observations: increased understanding of catchment processes through stepwise model improvement *Hydrol. Earth Syst. Sci.* **25** 957–82

Kaandorp V P, Molina-Navarro E, Andersen H E, Bloomfield J P, Kuijper M J and de Louw P G 2018 A conceptual model for the analysis of multi-stressors in linked groundwater–surface water systems *Sci. Total Environ.* **627** 880–95

Kim J P, Jung I W, Park K W, Yoon S K and Lee D 2016 Hydrological utility and uncertainty of multi-satellite precipitation products in the mountainous region of South Korea *Remote Sens.* **8** 608

Kirchner J W 2016 Aggregation in environmental systems–Part 1: seasonal tracer cycles quantify young water fractions, but not mean transit times, in spatially heterogeneous catchments *Hydrol. Earth Syst. Sci.* **20** 279–97

Kirchner J W, Feng X and Neal C 2000 Fractal stream chemistry and its implications for contaminant transport in catchments *Nature* **403** 524–7

Kirchner J W and Neal C 2013 Universal fractal scaling in stream chemistry and its implications for solute transport and water quality trend detection *Proc. Natl Acad. Sci.* **110** 12213–8

Knapp J L, Neal C, Schlumpf A, Neal M and Kirchner J W 2019 New water fractions and transit time distributions at Plynlimon, Wales, estimated from stable water isotopes in precipitation and streamflow *Hydrol. Earth Syst. Sci.* **23** 4367–88

Koeniger P, Wittmann S, Leibundgut C and Krause W 2005 Tritium balance modelling in a macroscale catchment *Hydrol. Process.: An Int. J.* **19** 3313–20

Kuppel S, Tetzlaff D, Maneta M P and Soulsby C 2020 Critical Zone Storage Controls on the Water Ages of Ecohydrological Outputs *Geophys. Res. Lett.* **47**

Li L *et al* 2017 Expanding the role of reactive transport models in critical zone processes *Earth Sci. Rev.* **165** 280–301

Maher K 2011 The role of fluid residence time and topographic scales in determining chemical fluxes from landscapes *Earth Planet. Sci. Lett.* **312** 48–58

Marschner P and Rengel Z 2023 Nutrient availability in soils *Marschner's Mineral Nutrition of Plants* (Elsevier) pp 499–522

McDonnell J J and Beven K 2014 Debates-The future of hydrological sciences: a (common) path forward? A call to action aimed at understanding velocities, celerities and residence time distributions of the headwater hydrograph *Water Resour. Res.* **50** 5342–50

McMillan H 2020 Linking hydrologic signatures to hydrologic processes: a review *Hydrol. Process.* **34** 1393–409

Molénat J, Gascuel-Odoux C, Aquilina L and Ruiz L 2013 Use of gaseous tracers (CFCs and SF6) and transit-time distribution spectrum to validate a shallow groundwater transport model *J. Hydrol.* **480** 1–9

Prenner D, Kaitna R, Mostbauer K and Hrachowitz M 2018 The value of using multiple hydrometeorological variables to predict temporal debris flow susceptibility in an alpine environment *Water Resour. Res.* **54** 6822–43

Remondi F, Kirchner J W, Burlando P and Fatichi S 2018 Water flux tracking with a distributed hydrological model to quantify controls on the spatio-temporal variability of transit time distributions *Water Resour. Res.* **54** 3081–99

Rinaldo A, Benettin P, Harman C J, Hrachowitz M, McGuire K J, Van Der Velde Y, Bertuzzo E and Botter G 2015 Storage selection functions: a coherent framework for quantifying how catchments store and release water and solutes *Water Resour. Res.* **51** 4840–7

Rodriguez N B, McGuire K J and Klaus J 2018 Time-varying storage–water age relationships in a catchment with a mediterranean climate *Water Resour. Res.* **54** 3988–4008

Schmidt A, Frank G, Stichler W, Duester L, Steinkopff T and Stumpp C 2020 Overview of tritium records from precipitation and surface waters in Germany *Hydrol. Process.* **34** 1489–93

Sivapalan M and Blöschl G 2015 Time scale interactions and the coevolution of humans and water *Water Resour. Res.* **51** 6988–7022

Solomon D, Gilmore T, Solder J, Kimball B and Genereux D 2015 Evaluating an unconfined aquifer by analysis of age-dating tracers in stream water *Water Resour. Res.* **51** 8883–99

Soulsby C, Birkel C and Tetzlaff D 2016 Characterizing the age distribution of catchment evaporative losses *Hydrol. Process.* **30** 1308–12

Sprenger M, Tetzlaff D, Buttle J, Laudon H and Soulsby C 2018 Water ages in the critical zone of long-term experimental sites in northern latitudes *Hydrol. Earth Syst. Sci.* **22** 3965–81

Stewart M K, Mehlhorn J and Elliott S 2007 Hydrometric and natural tracer (18O, silica, 3H and SF6) evidence for a dominant groundwater contribution to Pukemanga Stream, New Zealand *Hydrol. Process.* **21** 3340–56

Stewart M K, Morgenstern U and McDonnell J J 2010 Truncation of stream residence time: how the use of stable isotopes has skewed our concept of streamwater age and origin *Hydrol. Process.* **24** 1646–59

Stockinger M P, Bogena H R, Lücke A, Stumpp C and Vereecken H 2019 Time variability and uncertainty in the fraction of young water in a small headwater catchment *Hydrol. Earth Syst. Sci.* **23** 4333–47

Stockinger M P and Stumpp C 2024 Lessons learned from the spatiotemporal analysis of long-term and time-variable young water fractions of large central European river basins *Hydrol. Process.* **38** e15038

Thompson S E and Katul G G 2012 Multiple mechanisms generate Lorentzian and 1/fα power spectra in daily stream-flow time series *Adv. Water Resour.* **37** 94–103

Visser A, Thaw M, Deinhart A, Bibby R, Safeeq M, Conklin M, Esser B and Van der Velde Y 2019 Cosmogenic isotopes unravel the hydrochronology and water storage dynamics of the Southern Sierra Critical Zone *Water Resour. Res.* **55** 1429–50

von Freyberg J, Allen S T, Seeger S, Weiler M and Kirchner J W 2018 Sensitivity of young water fractions to hydro-climatic forcing and landscape properties across 22 Swiss catchments *Hydrol. Earth Syst. Sci.* **22** 3841–61

Wang S, Hrachowitz M and Schoups G 2024 Multi-decadal fluctuations in root zone storage capacity through vegetation adaptation to hydro-climatic variability has minor effects on the hydrological response in the Neckar basin, Germany *Hydrol. Earth Syst. Sci. Discuss.* **2024** 1–34

Wang S, Hrachowitz M, Schoups G and Stumpp C 2023 Stable water isotopes and tritium tracers tell the same tale: no evidence for underestimation of catchment transit times inferred by stable isotopes in StorAge Selection (SAS)-function models *Hydrol. Earth Syst. Sci.* **27** 3083–114

Weiler M, McGlynn B L, McGuire K J and McDonnell J J 2003 How does rainfall become runoff? A combined tracer and runoff transfer function approach *Water Resour. Res.* **39** 1315

Wilusz D C, Harman C J and Ball W P 2017 Sensitivity of catchment transit times to rainfall variability under present and future climates *Water Resour. Res.* **53** 10231–56

Wilusz D, Harman C, Ball W, Maxwell R and Buda A 2020 Using particle tracking to understand flow paths, age distributions, and the paradoxical origins of the inverse storage effect in an experimental catchment *Water Resour. Res.* **56** e2019WR025140

Zuber A 1986 On the interpretation of tracer data in variable flow systems *J. Hydrol.* **86** 45–57